Pseudo-Casimir force in confined nematic polymers

J. Dobnikar[2] and R. Podgornik[1,2](*)

[1] *Department of Physics, Faculty of Mathematics and Physics, University of Ljubljana
Jadranska 19, 1000 Ljubljana, Slovenia*
[2] *J. Stefan Institute, University of Ljubljana - Jamova 39, 1000 Ljubljana, Slovenia*

Abstract. – We investigate the pseudo-Casimir force in a slab of material composed of nematically ordered long polymers. We write the total mesoscopic energy together with the constraint connecting the local density and director fluctuations and evaluate the corresponding fluctuation free energy by standard methods. This leads to a pseudo-Casimir force of a different type than in the case of standard, short-molecule nematics. We investigate its separation dependence and its magnitude and explicitly derive the relevant limiting cases.

Casimir effect is due to constrained fluctuations in media with long-ranged correlations [1]. The physical nature of the medium is not particularly important. Though the standard Casimir effect has been introduced for constrained electromagnetic-field fluctuations, it has been realized that other systems with long-range correlations exhibit a similar type of fluctuation-driven interactions. Most notably critical fluids [1], smectic manifolds [2] and liquid crystals [3], all of them being prime examples of correlated fluids, give rise to a pseudo-Casimir effect which comes about through constrained thermal (as opposed to quantum) fluctuations of order parameters. The nature of these order parameters of course depends on the system under study but they all exhibit massless fluctuation spectra that eventually lead to long-ranged fluctuation interactions.

Limiting ourselves to the case of liquid crystals, the pseudo-Casimir effect has been researched in nematic, smectic and columnar uniformly ordered systems [3]. In the case of inhomogeneous or frustrated order as in the case of the hybrid-aligned cell characterized by opposing surface fields or in the Fréedericksz cell where frustration arises from competing bulk and surface fields [4], the interaction induced by director fluctuations is enhanced substantially by frustration, the enhancement being progressively stronger as the system approaches the transition from uniform to distorted structure.

There might be some experimental evidence that backs up these theoretical predictions [5] but we still lack a definitive experimental observation of the pseudo-Casimir interaction. It appears, however, that in the case of spinodal dewetting of 5CB on a silicon wafer [6] the pseudo-Casimir interaction is essential in giving a consistent interpretation of experimental

data, implying that this experiment can be regarded as the first observation of pseudo-Casimir effect in liquid crystals [7].

In this contribution we shall investigate the pseudo-Casimir effect in the realm of confined polymers. As a case study we will take a nematic polymeric liquid crystal such as one can observe in stiff polyelectrolytes above the isotropic-nematic transition, confined between two apposed planar surfaces. A physical realization of this case would be a nematically ordered DNA confined between two surfaces or simply cut to form a slab of macroscopically oriented sample [8] as is usually done in experiments with wet-spun DNA. We believe that this case is particularly instructive since we will be able to connect different limiting results with the existing calculations for ordinary, *i.e.* short chain, nematics [3]. It will be shown that the polymeric nature of the nematogens gives rise to additional features of the pseudo-Casimir effect that distinguish it qualitatively from results derived in the case of short nematogens. Also we will show that in the case of nematic polymers the pseudo-Casimir interaction depends on the equation of state [8] of the polymer nematic through its osmotic compressibility.

The elastic deformation of an ordinary short-molecule nematic [9] with long-range orientational order along the z-axis, can be described with an average director $\boldsymbol{n}(\boldsymbol{r})$, with small fluctuations in the (x, y)-directions: $\boldsymbol{n}(\boldsymbol{r}) \simeq (1, \delta n_x(\boldsymbol{r}), \delta n_y(\boldsymbol{r}))$. In this case, if the splay, twist and bend elastic constants are the Frank constants K_1, K_2 and K_3, one obtains for the mesoscopic elastic Hamiltonian

$$\mathcal{H}_{\boldsymbol{n}}[\delta \boldsymbol{n}(\boldsymbol{r})] = \frac{1}{2} \int \mathrm{d}^2 \boldsymbol{r}_\perp \mathrm{d}z \left[K_1 \left(\boldsymbol{\nabla}_\perp \cdot \delta \boldsymbol{n} \right)^2 + K_2 \left(\boldsymbol{\nabla}_\perp \times \delta \boldsymbol{n} \right)^2 + K_3 \left(\partial_z \delta \boldsymbol{n} \right)^2 \right]. \tag{1}$$

Besides fluctuations in nematic director, one should also consider fluctuations in the local density of the molecules. For short nematogens the director and density fluctuations are decoupled and one need not consider this part of the mesoscopic free energy explicitly. For long, polymer nematics the situation is altogether different. In this case we have to consider the part of the free energy due to nonhomogeneous density fluctuations $\rho(\boldsymbol{r}) \simeq \rho_0 + \delta\rho(\boldsymbol{r})$ in the Ornstein-Zernicke form

$$\mathcal{H}_\rho[\delta\rho(\boldsymbol{r})] = \frac{1}{2} \int \mathrm{d}^2 \boldsymbol{r}_\perp \mathrm{d}z \left[B \left(\frac{\delta\rho}{\rho_0} \right)^2 + B\xi^2 \left(\frac{\boldsymbol{\nabla}\delta\rho}{\rho_0} \right)^2 \right], \tag{2}$$

where B is the osmotic compressibility modulus and ξ is the density correlation length. Because polymers are here considered to be infinitely long, one also has to take into account the fact that director inhomogeneities can relax only if accompanied by the simultaneous density relaxation [10]. This leads to the constraint

$$0 = \boldsymbol{\nabla} \left(\rho\boldsymbol{n} \right) \simeq \partial_z \delta\rho + \rho_0 \left(\boldsymbol{\nabla}_\perp \cdot \delta\boldsymbol{n} \right). \tag{3}$$

Adding all the components of the mesoscopic free energy and taking the constraint equation (3) into account via a coupling constant, we obtain

$$\mathcal{H} = \mathcal{H}_{\boldsymbol{n}}[\delta\boldsymbol{n}] + \mathcal{H}_\rho[\delta\rho] + \frac{1}{2}C \int \mathrm{d}^2 \boldsymbol{r}_\perp \mathrm{d}z \left(\partial_z \delta\rho + \rho_0 \left(\boldsymbol{\nabla}_\perp \cdot \delta\boldsymbol{n} \right) \right)^2. \tag{4}$$

In general one can show [11] that the coupling constant equals $C = kT\ell/2\rho_\perp$, where $\rho_\perp$ is the average polymer density perpendicular to the nematic director and ℓ is a typical length of the polymers. For intrinsically stiff polymer chains like DNA, one can safely take $C \to \infty$ in accord with more microscopic calculations (see the discussion of this point in [11]).

Writing $\delta \boldsymbol{n}$ in the Helmholtz ansatz $\delta \boldsymbol{n} = \delta \boldsymbol{n}_\parallel + \delta \boldsymbol{n}_\perp$, we realize that the tangential part of the Hamiltonian is decoupled from the constraint eq. (3), giving the same contribution to the fluctuational free energy as in the case of short nematics [3].

Obviously in the case of polymer nematics the longitudinal director and the density field fluctuations are coupled. The fluctuational free energy is now obtained via

$$\mathcal{F} = -kT \ln \mathcal{Z} = -kT \ln \int_{\delta \boldsymbol{n}(\partial) = 0} \mathcal{D} \delta \boldsymbol{n} \int_{\delta \rho(\partial) = 0} \mathcal{D} \delta \rho \ \exp\left[-\beta \mathcal{H}\right], \tag{5}$$

where we have assumed that at the boundary of the sample the fluctuations in density and director field are quenched (*i.e.* $\delta \boldsymbol{n}(\partial) = 0, \delta \rho(\partial) = 0$). In principle one could also introduce the anchoring and tension energy of the bounding surfaces which would not bring any new qualitative features into our discussion but would make the computations less transparent.

We now analyze the fluctuational free energy of a slab of nematic material bounded at $z = \pm L/2$ where the average director is aligned with the z-axis. In the case of short nematogens ($C = 0$) the free energy decouples and we obtain two contributions: a long-range pseudo-Casimir free energy due to director fluctuations and a short-range term due to screened density fluctuations. Thus

$$\mathcal{F}(C = 0) = -\frac{kTS}{16\pi} \left(\frac{K_3}{K_1} + \frac{K_2}{K_1}\right) \frac{\zeta(3)}{L^2} - \frac{kTS}{16\pi} \frac{\epsilon(L/\xi)}{L^2}, \tag{6}$$

where S is the area of the surface, $\epsilon(x) = \int_x^\infty u \ \mathrm{d}u \ \ln\left(1 - e^{-u}\right)$ and $\zeta(n)$ Riemann's Zeta function. Since $L/\xi \gg 1$ and the function $\epsilon(x)$ has an exponential behavior for large values of the argument, the density fluctuations make a negligible contribution to the total free energy. Our result thus evidently reduces to the one obtained by Ajdari *et al.* [3].

In the case that the director and density fluctuations are coupled the calculation of the functional integral equation (5) becomes more complicated. First of all, we transform the Hamiltonian equation (4) by introducing

$$\delta \rho = \rho_0 \left(\boldsymbol{\nabla}_\perp \cdot \boldsymbol{a} + f\right), \qquad \delta \boldsymbol{n} = -\partial_z \boldsymbol{a} = -\dot{\boldsymbol{a}}. \tag{7}$$

The coupling term in this case reduces to

$$C \left(\partial_z \rho + \rho_0 \boldsymbol{\nabla}_\perp \cdot \delta \boldsymbol{n}\right)^2 \to C \rho_0^2 \left(\partial_z f\right)^2 = C' \dot{f}^2 \tag{8}$$

and the Hamiltonian is

$$\mathcal{H} = \frac{1}{2} \int \mathrm{d}^2 \boldsymbol{r}_\perp \mathrm{d}z \left[K_3 \ddot{\boldsymbol{a}}^2 + K_1 \left(\boldsymbol{\nabla}_\perp \dot{\boldsymbol{a}}\right)^2 + B \left(\boldsymbol{\nabla}_\perp \boldsymbol{a} + f\right)^2 + B\xi^2 \left(\boldsymbol{\nabla}_\perp (\boldsymbol{\nabla}_\perp \boldsymbol{a} + f)\right)^2 + \right.$$
$$\left. + B\xi^2 \left(\boldsymbol{\nabla}_\perp \dot{\boldsymbol{a}} + \dot{f}\right)^2 + C' \dot{f}^2 \right]. \tag{9}$$

Clearly in the limit of $C \longrightarrow \infty$, f becomes independent of z, thus $\dot{f} = 0$. In this case we can introduce the following linear transformation:

$$\boldsymbol{a} \longrightarrow \boldsymbol{a} + \boldsymbol{\nabla}_\perp A, \qquad \nabla_\perp^2 A = -f, \tag{10}$$

obtaining finally for the Hamiltonian in the limit of strong coupling

$$\mathcal{H} = \frac{1}{2} \int \mathrm{d}^2 \boldsymbol{r}_\perp \mathrm{d}z \left[K_3 \ddot{\boldsymbol{a}}^2 + K_1 \left(\boldsymbol{\nabla}_\perp \cdot \dot{\boldsymbol{a}}\right)^2 + B \left(\boldsymbol{\nabla}_\perp \cdot \boldsymbol{a}\right)^2 + B\xi^2 \left(\boldsymbol{\nabla}_\perp (\boldsymbol{\nabla}_\perp \cdot \boldsymbol{a})\right)^2 + B\xi^2 \left(\boldsymbol{\nabla}_\perp \cdot \dot{\boldsymbol{a}}\right)^2 \right]. \tag{11}$$

Since $\boldsymbol{a}$ is a longitudinal vector (eq. (7)), one obtains in the Fourier space

$$\mathcal{H} = \frac{1}{2} \sum_{\boldsymbol{Q}} \int \mathrm{d}z \left[K_3 \ddot{\boldsymbol{a}}_\parallel^2 + \left(K_1 + B\xi^2 \right) Q^2 \dot{\boldsymbol{a}}_\parallel^2 + B \left(1 + \xi^2 Q^2 \right) Q^2 \boldsymbol{a}_\parallel^2 \right]. \qquad (12)$$

The mesoscopic Hamiltonian obviously corresponds to a persistent oscillator, *i.e.* an oscillator with an additional fourth-order term in the derivatives. Since the different Fourier components are decoupled, the evaluation of the functional integral proceeds straightforwardly and can in fact be reduced to a Feynman integral for second-derivative Lagrangian solved exactly by Kleinert [12]. Taking into account the boundary conditions for the fluctuating fields, we obtain up to a multiplicative constant

$$\mathcal{Z} = \Pi_{\boldsymbol{Q}} \frac{(2\pi kT)^{-1} \sqrt{\omega_1 \omega_2} |\omega_1^2 - \omega_2^2| (\omega_1^2 + \omega_2^2)^{-1}}{\sinh(\omega_1 K_3^{-\frac{1}{3}} L) \sinh(\omega_2 K_3^{-\frac{1}{3}} L) - \frac{2\omega_1 \omega_2}{(\omega_1^2 + \omega_2^2)} (\cosh(\omega_1 K_3^{-\frac{1}{3}} L) \cosh(\omega_2 K_3^{-\frac{1}{3}} L) - 1)}, \qquad (13)$$

where

$$(\omega_1^2 + \omega_2^2) = \frac{1}{2} \left(K_1 + B\xi^2 \right) Q^2 K_3^{-1/3},$$

$$(\omega_1 \omega_2)^2 = B \left(1 + \xi^2 Q^2 \right) Q^2 K_3^{1/3}. \qquad (14)$$

Introducing now $\Omega_\pm = K_3^{-1/3}(\omega_1 \pm \omega_2)$ and with

$$\Omega_\pm^2(Q) = \frac{K_1 + B\xi^2}{2K_3} Q \left[Q \pm 4\Lambda \sqrt{1 + \xi^2 Q^2} \right], \qquad (15)$$

where

$$\Lambda = \frac{\sqrt{BK_3}}{K_1 + B\xi^2}, \qquad (16)$$

we obtain, for the regularized fluctuation, the free energy per unit area, where the formally divergent bulk and surface free-energy terms have already been subtracted:

$$\mathcal{F} = \frac{kTS}{4\pi} \int_0^\infty Q\mathrm{d}Q \ln \left(1 - 2\frac{\Omega_+^2}{\Omega_-^2} e^{-\Omega_+ L} \left[\cosh(\Omega_- L) - \frac{\Omega_+^2 - \Omega_-^2}{\Omega_+^2} \right] + e^{-2\Omega_+ L} \right). \qquad (17)$$

In the above equations Ω_-^2 can become negative for sensible values of the correlation length ξ. In this case the $\cosh \Omega_- L$ has to be replaced by $\cos |\Omega_-| L$ but the integral contains no dangerous divergencies and can be evaluated straightforwardly. By introducing

$$\mathcal{F}^* = \frac{kTS}{4\pi} \Lambda^2 \quad \text{and} \quad L^* = \sqrt{\frac{2(K_1 + B\xi^2)}{B}}, \qquad (18)$$

we realize that the dimensionless free energy $\mathcal{F}/\mathcal{F}^*$ obtained from eq. (17) depends only on the dimensionless separation L/L^* and the dimensionless coupling constant $\gamma = \Lambda\xi$. This coupling constant basically represents the ratio between the density correlation length ξ and the polymer nematic correlation length perpendicular to the average director Λ^{-1} [8].

In order to estimate the magnitude of the pseudo-Casimir forces in confined nematic polymers, we now have to connect the macroscopic elastic constants K_1, K_3, B and the correlation
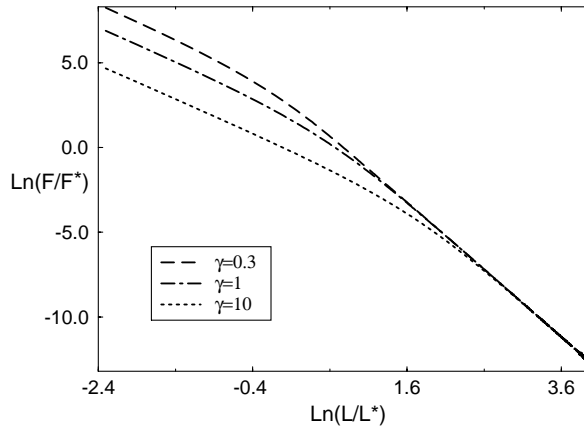
Fig. 1 – The dependence of the dimensionless free energy $\frac{\mathcal{F}}{\mathcal{F}^*}$ on the dimensionless separation $\frac{L}{L^*}$ obtained from eq. (17) for different values of the coupling constant γ. The two scaling regimes at small and large $\frac{L}{L^*}$ are clearly visible.

length ξ with the microscopic interaction parameters of the systems. This is in general a very difficult undertaking. For DNA this type of analysis has been performed in [8,13] and we use these results in what follows.

If the interaction potential between the segments of the polymers is $U(D)$, where D is the average spacing between the molecules perpendicular to the average director and the intrinsic persistence length of the polymers is $\mathcal{L}_P$, one has [8]

$$K_1 = K_2 \simeq U(D)/D\,,$$

$$K_3 \simeq kT\,\mathcal{L}_P\,\rho_\perp + U(D)/D\,,$$

$$B \simeq \frac{\sqrt{3}}{4}\left(\frac{\partial^2}{\partial D^2} - \frac{1}{D}\frac{\partial}{\partial D}\right)U(D)/\mathcal{L}_P\,. \tag{19}$$

One should realize here that since DNA is a polyelectrolyte, the interaction potential $U(D)$ is composed of two additive parts: the short-ranged hydration part and the longer-ranged screened Coulomb part (for details see [8]). The latter of course depends on the ionic strength of the bathing solution. Both contributions to $U(D)$ decay exponentially with D [8], but with different decay lengths.

The above scaling of elastic constants leads to the conclusion that $\frac{K_2}{K_1} \sim 1$ and $\frac{K_3}{K_1} \gg 1$, the latter due to the fact that DNA has an intrinsic elastic modulus that contributes a term independent of $U(D)$ to K_3, see eq. (19).

Figure 1 presents a plot of the dimensionless free energy as a function of dimensionless separation. The curves are plotted for various values of the coupling constant γ which is plotted as a function of the average spacing between polymers in fig. 2 for the case of DNA. One can clearly discern two regions with approximately L^{-2} and L^{-4} behavior separated by a characteristic spacing $L_0 = C(\gamma)L^*$, where $C(\gamma)$ is a numerical factor depending on the coupling constant that can be read off fig. 1. The characteristic spacing L_0 grows approximately linearly with the average separation between the polymers D, ranging from about 20 nm at $D = 2$ nm to around 150 nm at $D = 8$ nm, which amounts to between one and two correlation lengths ξ [13].
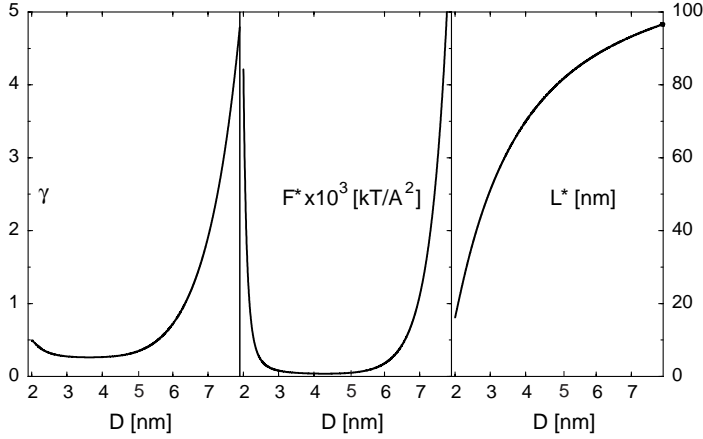
Fig. 2 – The dependence of the magnitude of the pseudo-Casimir interaction $\mathcal{F}^*$, the characteristic length L^* and the coupling constant γ on the average separation between the polymers obtained via the interaction potential $U(D)$ and ξ taken from [8, 13] in the case of 0.5 M NaCl bathing ionic solution. Note that γ and $\mathcal{F}^*$ have the same scale. L^* saturates for small values of DNA density (large D) at about 140 Å.

Figure 2 shows the dependence of the magnitude of the pseudo-Casimir interaction $\mathcal{F}^*$, the characteristic length L^* and the coupling constant γ on the average separation between the polymers obtained from the measured equation of state for DNA in the case of 0.5 M bathing solution of NaCl (for details see [8]).

One would of course like to have also approximate analytical formulae for the pseudo-Casimir interaction eq. (17). There are only two limiting cases where the integral in eq. (17) can be evaluated analytically, the large-separation and the small-separation regime. First of all for small L the dominant behavior of the integral is obtained at large Q leading in this case to

$$\mathcal{F}(L \ll L_0) = -\frac{kTS}{16\pi L^2} \left(\frac{K_3}{K_1 \left(1 + 4\Lambda\xi\right) \cdot \left(1 + \frac{B}{K_1}\xi^2\right)} + \frac{K_2}{K_1} \right) \zeta(3). \tag{20}$$

Thus $\mathcal{F}(L \ll L_0)$ depends on L just as in the case of a standard nematic [3]. Its magnitude can, however, in the case of small polymer density or equivalently large D (small K_1, K_2), substantially exceed the pseudo-Casimir force in standard nematics due to the intrinsic stiffness term in the elastic constant K_3, eq. (19). In this case

$$\mathcal{F}(L \ll L_0; K_1, K_2 \to 0) = -\frac{kTS}{64\pi\xi L^2} \sqrt{\frac{K_3}{B}} \; \zeta(3). \tag{21}$$

Also because for $L \ll L_0$ the L dependencies are the same, it is reasonable to compare the pseudo-Casimir interaction with the van der Waals interaction. From eq. (20) one can show that their ratio scales approximately as $\mathcal{F}(L \ll L_0)/\mathcal{F}_{\mathrm{vdW}} \gtrsim (K_3 kT/K_1 H)$ for large D and as $\gtrsim \sqrt{\frac{K_3}{B}}(kT/H\xi)$ for small D. H is the Hamaker constant. In the case of an intrinsically stiff polymer such as DNA with K_3 as in eq. (19) both of these ratios are much larger than 1.

The other analytically tractable limit is in the case of large L where the dominant contribution to the integral comes from small-Q behavior of the integrand

$$\mathcal{F}(L \gg L_0) = -\frac{kTS}{16\pi} \left[\frac{2K_3\zeta(5)}{BL^4} + \frac{K_2\zeta(3)}{K_1L^2} \right], \qquad (22)$$

where the length scale L_0 can be read off the graph in fig. 1 for various values of γ (see above). For large L the dependence of the pseudo-Casimir interaction free energy on L is altogether different, deviating essentially from the standard nematic case. The crossover between the two regimes moves to larger L as the polymers become less dense (see fig. 2) but eventually saturates for small polymer densities.

The pseudo-Casimir interaction for long nematic polymers thus differs qualitatively from the one obtained in the case of short nematics [3]. Though it still decays algebraically with L, and thus qualifies as a long-range force, it decays asymptotically faster (L^{-4}) than in the case of short nematics (L^{-2}). Nevertheless its absolute magnitude can, depending on the polymer density and the regime of spacings L, become comparable to and even much larger than that in the case of short nematics with numerically comparable Frank constants (though possibly stemming from different microscopic interactions). The L^{-4} behavior stems essentially from the polymer stiffness and should thus be a salient feature of the pseudo-Casimir interactions whenever the mesoscopic Hamiltonian contains the squares of higher than the first derivatives in the order parameter. These types of systems will be studied in our future work.

$$* * *$$

REFERENCES

[1] Mostepanenko V. M. and Trunov N. N., *The Casimir Effect and its Applications* (Clarendon Press, Oxford) 1997.
[2] Li H. and Kardar M., *Phys. Rev. Lett.*, **67** (1991) 3275; *Phys. Rev. A*, **46** (1992) 6490.
[3] Ajdari A., Peliti L. and Prost J., *Phys. Rev. Lett.*, **66** (1991) 1481; Ajdari A., Duplantier B., Hone D., Peliti L. and Prost J., *J. Phys. II*, **2** (1992) 487.
[4] Ziherl P., Karimi Pour Haddadan F., Podgornik R. and Žumer S., *Phys. Rev. E*, **61** (2000) 5361.
[5] Swanson B. D. and Sorensen L. B., *Phys. Rev. Lett.*, **75** (1995) 3293.
[6] Vandenbrouck F., Valignat M. P. and Cazabat A. M., *Phys. Rev. Lett.*, **82** (1999) 2693.
[7] Ziherl P., Podgornik R. and Žumer S., *Phys. Rev. Lett.*, **84** (2000) 1228.
[8] Strey H. H., Parsegian V. A. and Podgornik R., *Phys. Rev. E*, **59** (1999) 999.
[9] de Gennes P. G. and Prost J., *The Physics of Liquid Crystals* (Clarendon Press, Oxford) 1993.
[10] de Gennes P. G., *Mol. Cryst. Liq. Cryst. Lett.*, **34** (177) 1977.
[11] Kamien R. D., Le Doussal P. and Nelson D. R., *Phys. Rev. A*, **45** (1992) 8727.
[12] Grosche C. and Steiner F., *Handbook of Feynman path integrals, Springer Tracts Mod. Phys.*, Vol. **145** (Springer, New York) 1998.
[13] Strey H. H., Wang J., Podgornik R., Rupprecht A., Yu L., Parsegian V. A. and Sirota E., *Phys. Rev. Lett.*, **84** (2000) 3105.